Composites Part B 83 (2015) 194–202

Contents lists available at ScienceDirect

Composites Part B

journal homepage: www.elsevier.com/locate/compositesb

Bending stiffening of graphene and other 2D materials via controlled rippling

E. Jomehzadeh [a, *], N.M. Pugno [b, c, d, **]

[a] Department of Mechanical Engineering, Graduate University of Advanced Technology, Kerman, Iran
[b] Laboratory of Bio-inspired & Graphene Nanomechanics, Department of Civil, Environmental and Mechanical Engineering, University of Trento, Trento, Italy
[c] Center for Materials and Microsystems, Fondazione Bruno Kessler, Povo, Trento, Italy
[d] School of Engineering & Materials Science, Queen Mary University of London, London, UK

ARTICLE INFO

Article history:
Received 18 September 2014
Received in revised form
15 May 2015
Accepted 7 August 2015
Available online 14 August 2015

Keywords:
A. Nano-structures
B. Mechanical properties
C. Analytical modelling

ABSTRACT

In this paper, the effects of rippling on the bending stiffness of a monolayer graphene are studied. The initial rippling of the surface is modeled by cosine functions with a hierarchical topology. Considering both large displacement and small scale effect, the governing equilibrium equations are determined and solved. Then an equivalent bending stiffness is calculated for a rippled graphene and the effects of rippling, material discreteness, and structural dimension on its stiffness are discussed in details. The results quantify how the rippling strongly increases the effective bending stiffness of graphene and interacts with the discrete nature of the material not only because of increase in the moment of inertia. This approach can be applied to ripples design of 2D materials in order to achieve stiffening in bending as required in specific applications.

1. Introduction

Graphene is a novel material with remarkable mechanical, thermal and electrical properties and one of the strongest materials tested in terms of elastic modulus and tensile strength [1,2]. Although monolayer graphene has an exceptional stiffness, it is easily warped in out-of-plane direction and exhibits ripples [3] and folds [4]. A detailed analysis beyond the harmonic approximation proved that the coupling between bending and stretching modes stabilizes the atomical thin membranes through deformations in the third dimension called ripples [5]. In studies by Transmission Electron Microscopy (TEM), it has been shown that the freely suspended graphene sheets are not perfectly flat and exhibits intrinsic microscopic roughening with out of plane displacement up to 1 nm [5].

Due to the large computational expenses of nano-structures analyses when using atomic lattice dynamics and molecular dynamic simulations [6], there is a great interest in applying quasi-continuum mechanics to explain size effects at the nano-scale [7]. There are several articles in the literature that studied the linear analysis of graphene sheets and nanotubes based on the quasi-continuum mechanics [8–12]. The linear vibration [13–15], buckling [16,17] and wave propagation [18] analyses of graphene sheet were studied using nonlocal elasticity theory. Also, Jomehzadeh and Saidi [19] decoupled the three dimensional nonlocal equations of nanoplates considering the length scale effect.

In reality, no physical system is strictly linear and hence the linear models of physical systems have their own limitations. In general, linear models are only restrictively applicable when the amplitude is very small. Thus, in order to accurately identify and understand the behavior of a nano-structural system under general loading conditions, it is also essential to model the nonlinearities of the system. Xu and Liao [20] investigated the elastic response of a circular single layered graphene sheet under a transverse central load using molecular dynamics and continuum mechanics. They found that the continuum mechanics can yield predictions close to the molecular mechanics under large deformation for certain loading configurations, when modes of deformation are similar. A theoretical framework of nonlinear continuum mechanics was developed by Lu and Huang [21] for a graphene sheet under both in-plane and bending deformation. They have shown that graphene becomes highly nonlinear and anisotropic under finite strain

* Corresponding author. Department of Mechanical Engineering, Graduate University of Advanced Technology, Kerman, Iran.
** Corresponding author. Laboratory of Bio-inspired & Graphene Nanomechanics, Department of Civil, Environmental and Mechanical Engineering, University of Trento, Trento, Italy.
E-mail addresses: e.jomehzadeh@kgut.ac.ir (E. Jomehzadeh), nicola.pugno@unitn.it (N.M. Pugno).

http://dx.doi.org/10.1016/j.compositesb.2015.08.002
1359-8368/

uniaxial stretch, and the coupling between stretch and shear exists except for stretching in the zigzag and armchair directions. Duan and Wang [22] studied the deformation of a single layered circular graphene sheet under a central point load by using molecular mechanics and nonlinear plate theory. They found that, with properly selected parameters, the von Karman plate theory can provide a remarkably accurate prediction of the graphene sheet behavior under linear and nonlinear bending and stretching. Rezaei Mianroodi et al. [23] studied the nonlinear vibrational properties of single layer graphene sheets using a membrane model. The nonlinear equation of motion was obtained for graphene including the effects of stretching due to large amplitudes.

Wang [24] presented molecular mechanics simulations for bending rigidity of a graphene by calculations of its strain energy subjected to a point loading. The rigidity was found to be dependent on the size, deflection and shape of graphene. Considering the small scale effect, postbuckling, nonlinear bending and nonlinear vibration analyses were presented for simply supported stiff thin films in thermal environments [25,26]. Also, Jomehzadeh and Saidi [27] studied the large amplitude free vibration of multi layered graphene sheets using the nonlocal elasticity.

Graphene is intrinsically non-flat and tends to be corrugated due to the instability of two-dimensional crystals. Since the deformation of graphene can strongly affect its properties and the performance of graphene-based devices and materials [28], it is highly desirable to obtain and control the stiffness of a wrinkled graphene. Also, since graphene sheets can undergo large displacement within the elastic limit, the nonlinear analysis is clearly essential. Although some researchers studied the rippling of graphene [29–31], the effects of length scale and geometrical nonlinearity on the stiffness of a rippled graphene have not yet investigated. In this article, the changes of bending–stretching stiffness due to wrinkling are investigated for a monolayer graphene. In order to consider the bending–stretching coupling, nonlinear equations of large displacement are taken into account and an equivalent size-dependent bending stiffness is obtained for a rippled graphene. The effects of initial amplitude and frequency of surface on the bending stiffness of a rippled graphene are quantified and compared with the predictions based on the bending moment of inertia for the first time.

2. Surface wrinkling

Description of the surface topography is important in applications involving contact, friction, lubrication, and wear. The same concept of the roughness has statistical implications as it considers some factors such as sampling size and interval. In order to describe the effect of roughness, three general mathematical surface modeling techniques can usually be used, fractal geometry, Fourier transforms and sinusoidal function. A fractal surface is continuous but non-differentiable and can be represented by Weierstrass–Mandelbrot (W–M) function for one dimensional problems [32]. In fact, the real part of W–M fractal function is a superposition of cosines with geometrically spaced frequencies and amplitudes that obey a power law. Moreover, the essence of the Fourier transform of a wave form is to decompose or separate it into a sum of sinusoids of the different frequencies. Therefore, it is quite reasonable to model the roughness of the surface by the composition of trigonometric functions and it is a simplified model of the surface profile.

Let us consider a graphene sheet that is not initially flat with projection of dimensions l_1 and l_2 in x_1 and x_2 directions and thickness l_3 (Fig. 1). The Cartesian coordinate system is fixed at the center of the middle plane in its undeformed state. In order to model the wrinkling of the surface, we consider cosine terms with arbitrary amplitudes and frequencies as

$$u^0(x_1,x_2)=\sum_{k=1}^{N} l_3 \mathrm{A}_k \cos\left(\frac{n_{1k}\pi x_1}{l_1}\right)\cos\left(\frac{n_{2k}\pi x_2}{l_2}\right) \tag{1}$$

where $\mathrm{A_k}$ are the amplitudes of the wrinkling and parameters n_{1k} and n_{2k} are the frequencies of the surface roughness in x_1 and x_2 directions, respectively. By changing the frequencies and amplitudes, several models for surface rippling can be obtained. For example, the configuration of the surface with $N = 2$ is shown in Fig. 2 and it can be seen that this expression is capable of modeling a wide range of initial ripple modes even with $N = 2$.

3. Governing equations

Thanks to the thin lateral dimension of graphene sheets, the Kirchhoff hypotheses [33] for displacement of graphene are applicable. Therefore, the displacement components of a rippled graphene can be represented as

$$U_\alpha = u_\alpha - x_3 u_{3,\alpha}, \quad U_3 = u^0 + u_3 \tag{2}$$

where $u_\alpha = u_\alpha(x_1, x_2)$ are the displacement components at the middle plane and x_3 is the transverse direction. A comma stands for differentiation with respect to the suffix index and the α can be 1 or 2. In whole of the article the Greek subscripts changes from 1 to 2. As described in Eq. (1), u^0 is the initial displacement of the midplane in transverse direction due to existence of the surface rippling.

Since the linear theories are suitable only for infinitesimal displacement of structures, it is recommended to use nonlinear geometrical theories for large displacement of graphene [21,22]. Therefore, here the theory of large deflection of von Karman is considered. In von Karman theory, nonlinear terms that depend on u_3 are retained, therefore the Green strain components of this theory are expressed as [34].

$$\varepsilon_{\alpha\beta} = \left(u_{\alpha,\beta} + u_{\beta,\alpha} + u_{3,\alpha}u_{3,\beta} + 2u_{3,\alpha}u^0_{,\beta}\right)\Big/2 - x_3 u_{3,\alpha\beta}, \tag{3}$$

In order to describe the long-range interatomic interactions in nano-scale materials and express the results in term of the size of body, the nonlocal theory of elasticity can be used. The theory of nonlocal elasticity was first extensively developed from the early seventies in the last century [35]. The theory states that the stress at a point in a body depends not only on the classical local strain at that particular point but also on the spatial integrals with weighted averages of the local strain contribution of all other points in the body. Therefore, the nonlocal constitutive equations have the following form

$$\sigma_{\alpha\beta}(x) = C_{\alpha\beta\gamma\lambda}\varepsilon_{\gamma\lambda} + \int c_{\alpha\beta\gamma\lambda}(x,x')\varepsilon_{\gamma\lambda}(x')\mathrm{d}x' \tag{4}$$

where $\sigma_{\alpha\beta}$ is the nonlocal stress component, $\varepsilon_{\alpha\beta}$ strain component and $C_{\alpha\beta\gamma\lambda}$ the elastic coefficient of material.

The nonlocal effect is thus indented through the introduction of a nano-scale which depends on the material internal characteristic length and can capture the discreteness of the material. This internal length has no influence at macro-scale where the structure size is much bigger and hence the nonlocal effect vanishes for classical mechanics. Since the nonlocal stress components ($\sigma_{\alpha\beta}$) are related to strains components ($\varepsilon_{\gamma\lambda}$) by an integral form, the governing equations are expressed in integro-differential equations. Due to the integral form of the nonlocal stress, its final equations are more difficult to solve with respect to the differential form. An exact or approximate solution for the nonlocal integral function can

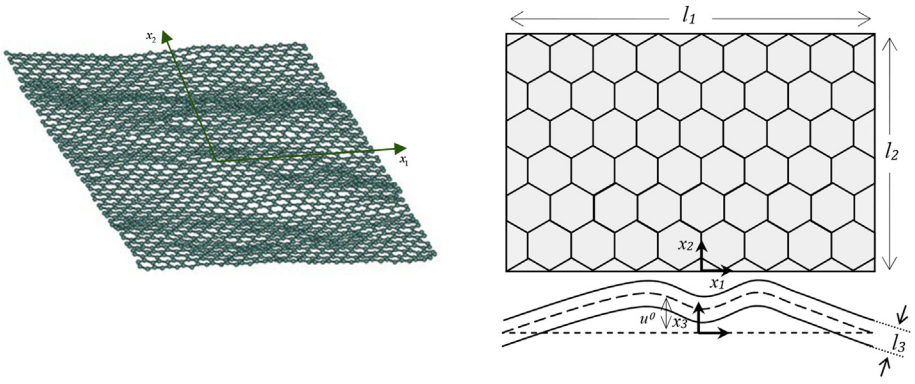

Fig. 1. The geometry of a rippled graphene.

be determined in some very special circumstances using the Green function and hence its use is rather limited. However, Eringen [36] presented an equivalent expression of the nonlocal stress in an equivalent differential form for nonlocal stress components as

$$\left[1-(e_0a)^2\nabla^2\right]\sigma_{\alpha\beta}=C_{\alpha\beta\gamma\lambda}\varepsilon_{\gamma\lambda} \tag{5}$$

where $(e_0a)^2=\mu$ is a small length scale or nonlocal parameter, e_0 is a numerical constant to adjust the model to match the reliable experimental results, a is an internal characteristic length such as C–C bond length or wave length and $\nabla^2=()_{,11}+()_{,22}$ is the Laplacian operator. Also, the Greek subscript can be 1 or 2. The nonlocal effect is presented through the introduction of a nonlocal length scale (μ) which depends on the material and internal characteristic length [8]. The ratio between nonlocal length scale to structural size goes to zero at macro-scale and hence the nonlocal effect vanishes in the limit of large structures recovering the classical mechanics. It was noted that the equilibrium equations have the same form for local and nonlocal theories [37]. However, the resultant forces and moments of the nonlocal theory contain small scale effect. In fact, these parameters are defined in terms of nonlocal stress and not local one as

$$N_{\alpha\beta}=\int_{-l_3/2}^{l_3/2}\sigma_{\alpha\beta}\,\mathrm{d}x_3,\quad M_{\alpha\beta}=\int_{-l_3/2}^{l_3/2}\sigma_{\alpha\beta}x_3\,\mathrm{d}x_3 \tag{6}$$

in which $\sigma_{\alpha\beta}$ has been defined in Eq. (5). $N_{\alpha\beta}$ and $M_{\alpha\beta}$ are the intensities of forces and moments, i.e., forces and moments per unit length of the midplane.

It should be noted that the properties of the graphene depend on the direction of chiral angle and they should be modeled as an anisotropic directionally dependent material. Obtaining the resultant forces and moments for an anisotropic graphene with considering the small scale effect, the nonlocal nonlinear governing equilibrium equations for a monolayer orthotropic graphene sheet can be obtained as [38]:

$$\begin{aligned}&D_{11}u_{3,1111}+2(D_{12}+2D_{33})u_{3,1122}+D_{22}u_{3,2222}\\&=\left(1-(e_0a)^2\nabla^2\right)P(x_1,x_2)+\left(1-(e_0a)^2\nabla^2\right)\\&\quad\times\left(\left(u^0+u_3\right)_{,11}\varphi_{,22}-2\left(u^0+u_3\right)_{,12}\varphi_{,12}\right.\\&\quad\left.+\left(u^0+u_3\right)_{,22}\varphi_{,11}\right)\end{aligned} \tag{7a}$$

$$\begin{aligned}&A_{11}\varphi_{,1111}+2(A_{12}+2A_{33})\varphi_{,1122}+A_{22}\varphi_{,2222}\\&=u_{3,12}u_{3,12}-u_{3,11}u_{3,22}+2u_{3,12}u^0_{,12}-u_{3,11}u^0_{,22}-u_{3,22}u^0_{,11}\end{aligned} \tag{7b}$$

where $P(x_1, x_2)$ is the external pressure in transverse direction and D_{ij} is the bending stiffness of graphene

$$D_{ij}=\int_{-l_3/2}^{l_3/2}Q_{ij}x_3^2\,\mathrm{d}x_3 \tag{8}$$

in which Q_{ij} is the plane-stress material constants and the subscripts i and j changes from 1 to 3. Since the thickness of graphene is thin and the initial deflection is small than the thickness, the plane-stress state can be assumed for its modeling [13,25]. The parameters A_{ij}, D_{ij} and Q_{ij} are defined in Appendix A in terms of material properties of graphene sheet. Also, the stress function φ is defined as

$$N_{11}=\varphi_{,22},\quad N_{22}=\varphi_{,11},\quad N_{12}=-\varphi_{,12} \tag{9}$$

where N is the resultant force defined in Eq. (6). As it can be seen, the governing equations (7) are two nonlinear partial differential equations in terms of the transverse deflection and stress function.

4. Solution

Let us consider the large deflection of a graphene sheet with uneven surface subjected to a constant pressure in transverse direction. It is assumed that the sheet has either hinged or clamped edges in which the conditions can be written as

$$\begin{aligned}&\text{at}\,x_1=\pm\frac{l_1}{2}:\begin{cases}\text{Hinged}: u_3=0, M_{11}=0, \varphi_{,12}=0, \displaystyle\int_{-l_2/2}^{l_2/2}\varphi_{,22}\,\mathrm{d}x_2=0\\ \text{Clamped}: u_3=0, u_{3,1}=0, \varphi_{,12}=0, \displaystyle\int_{-l_2/2}^{l_2/2}\varphi_{,22}\,\mathrm{d}x_2=0\end{cases}\\&\text{at}\,x_2=\pm\frac{l_2}{2}:\begin{cases}\text{Hinged}: u_3=0, M_{22}=0, \varphi_{,12}=0, \displaystyle\int_{-l_1/2}^{l_1/2}\varphi_{,11}\,\mathrm{d}x_1=0\\ \text{Clamped}: u_3=0, u_{3,2}=0, \varphi_{,12}=0, \displaystyle\int_{-l_1/2}^{l_1/2}\varphi_{,11}\,\mathrm{d}x_1=0\end{cases}\end{aligned} \tag{10}$$

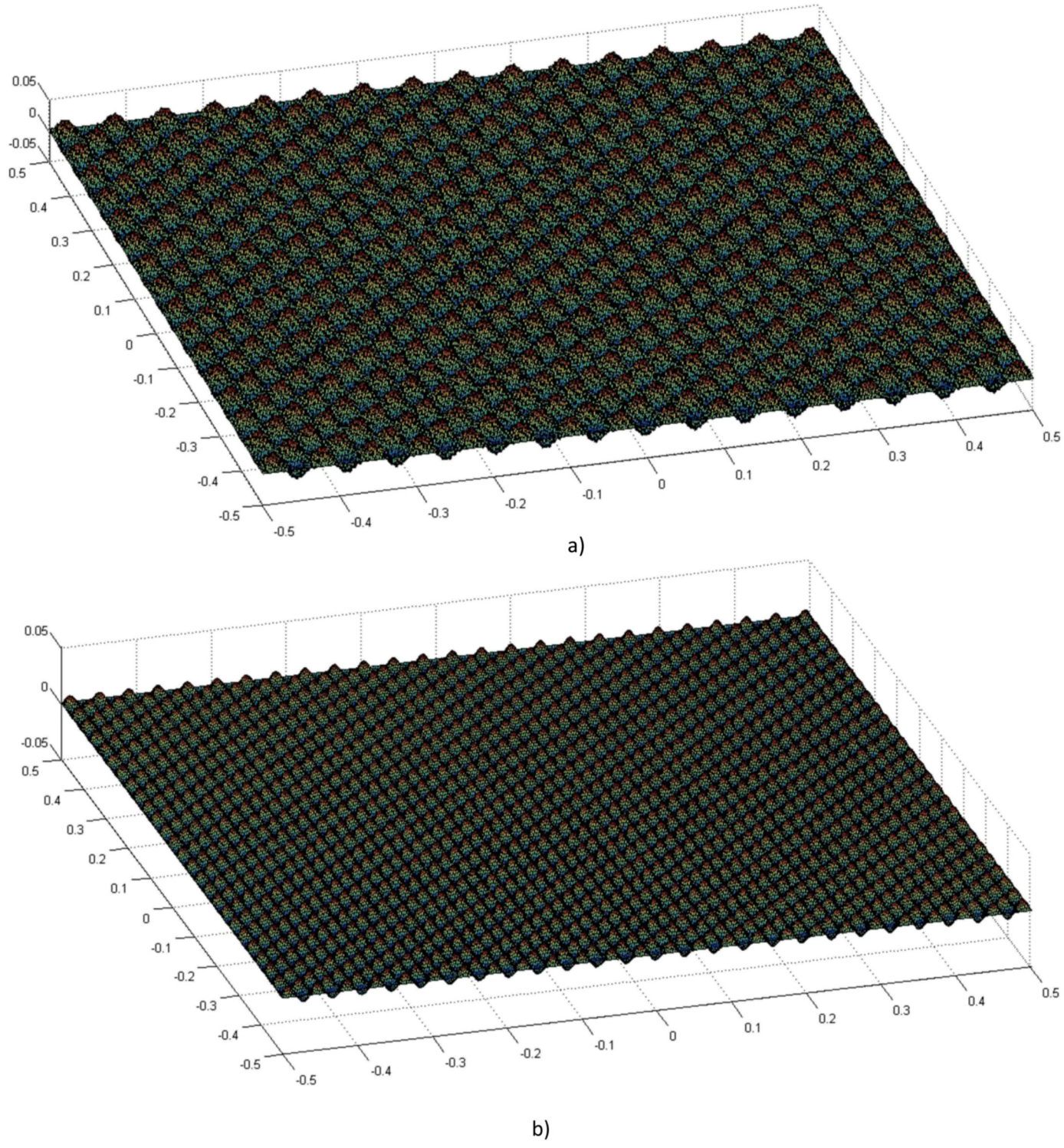

Fig. 2. Two samples of rippled graphene: a) $n_{11} = n_{21} = 31$, $n_{12} = n_{22} = 201$, b) $n_{11} = n_{21} = 51$, $n_{12} = n_{22} = 101$.

Regarding to these boundary conditions and loading pressure, the transverse deflection can be assumed in the following form

$$\text{For hinged graphene } u_3(x_1,x_2) = l_3 u_3 \cos\left(\frac{\pi x_1}{l_1}\right)\cos\left(\frac{\pi x_2}{l_2}\right) \tag{11a}$$

$$\text{For clamped graphene } u_3(x_1,x_2) = l_3 u_3 \cos^2\left(\frac{\pi x_1}{l_1}\right)\cos^2\left(\frac{\pi x_2}{l_2}\right) \tag{11b}$$

Substituting Eq. (11) into Eq. (7b) and considering the initial configuration as given by Eq. (1), the general solution for the stress

function φ can be obtained. Substituting the resulting stress function into Eq. (7a) and applying Galerkin's technique [39], one can obtain a single algebraic equation as follow

$$u_3^3 + \lambda_1 u_3^2 + \lambda_2 u_3 + \lambda_3 = 0 \tag{12}$$

where λ_1, λ_2 and λ_3 are three coefficients which depend on the material properties and geometric parameters. By obtaining the amplitude u_3 from the above equation and putting the result into Eq. (11), the transverse deflection of a graphene layer with an initial rippling can be defined.

5. Closed form solution

To understand the effects of nonlocality and rippling more clearly, a closed form solution is obtained for a special case. To this end, a square graphene ($l_1 = l_2 = l$) with isotropic material properties is considered. For this case, the relation between external pressure and transverse deflection of a rippled graphene is obtain as

$$P = \frac{\pi^6 l_3 D}{4l^4}\left\{\left(1+\sum_{i=k}^{N}\frac{3n_{1k}^2 n_{2k}^2}{2(n_{1k}n_{2k}+1)^2}\left(1-\nu^2\right)\left(1+2\pi^2\frac{\mu}{l^2}\right)A_k^2\right)u_3 + \frac{3}{8}\left(1-\nu^2\right)\left(1+2\pi^2\frac{\mu}{l^2}\right)u_3^3\right\} \tag{13}$$

where $D = El_3^3/12(1-\nu^2)$ is the bending stiffness of the classical theory, E and ν are Young modulus and Poisson's ratio of the isotropic graphene, respectively. It can be seen that the relation is nonlinear with respect to graphene deflection (u_3) therefore it can capture the large displacement. It is easily verified that for a flat and linear classical case ($A_k = 0,\ u_3^3 = 0,\ \mu = 0$), Eq. (13) becomes the prediction of the classical plate theory [40].

As it is seen from Eq. (13), the external pressure is related to the non-dimensional deflection (u_3), with two coefficients which represent the stiffness of graphene. The coefficients of u_3 and u_3^3 indicate the effects of bending stiffness and stretching–bending stiffness, respectively. It can be seen that the bending stiffness of graphene increases by square power of rippling amplitude (A_i). However, the bending–stretching stiffness is not related to initial rippling. It can be said that when a flat graphene wrinkles, its stretching or in-plane stiffness decreases while its bending stiffness increases. In our case, the invariant of stretching–bending stiffness due to uneven surface indicates that these two effects neutralize each other. Also, it can be seen that the initial rippling of graphene causes increase in the stiffness. It can be concluded that the nonlocal parameter plays a significant role in a rippled graphene.

Based on the Eq. (13), an equivalent bending stiffness for a square rippled graphene can be obtained as

$$D_{eq} = \left(1+\sum_{k=1}^{N}\frac{3n_{1k}^2 n_{2k}^2}{2(n_{1k}n_{2k}+1)^2}\left(1-\nu^2\right)\left(1+2\pi^2\frac{\mu}{l^2}\right)A_k^2 + \frac{3}{8}\left(1-\nu^2\right)\left(1+2\pi^2\frac{\mu}{l^2}\right)u_3^2\right)D \tag{14}$$

and for the linear case ($u_3^2 = 0$), it becomes

$$D_{eq} = \left(1+\sum_{i=1}^{N}\frac{3n_{1k}^2 n_{2k}^2}{2(n_{1k}n_{2k}+1)^2}\left(1-\nu^2\right)\left(1+2\pi^2\frac{\mu}{l^2}\right)A_k^2\right)D \tag{15}$$

To understand the changes of the bending stiffness due to wrinkling, the equivalent linear bending stiffness of simply supported rippled graphene to its flat counterpart ($\overline{D}$), is depicted in Fig. 3 for one term wrinkling ($N = 1$) and equal wave numbers in the two directions ($n_{11} = n_{21} = n$). It can be seen that the bending stiffness of a rippled graphene is more rigid than a flat one.

Variation of the bending stiffness ratio versus the surface roughness frequency is shown in Fig. 4 for several length scale parameters. It can be seen that the frequency of surface wrinkling has considerable effects on the bending stiffness of graphene and it causes a rapid increase in stiffness at low values of length scale. It can be seen that the variation of stiffness converges to a specific value of frequency and after that increase in surface frequency does not significantly change the graphene stiffness. Since the projection length of graphene (l) is constant, increase the frequency of surface roughness causes an increase in the graphene length and this decreases its stiffness. At higher frequencies, decrease of stiffness due to the length elongation counteracts the increase in the stiffness due to rippling.

As a flat surface of the graphene changes to an uneven surface, length of graphene decreases to keep constant surface area. A crumpled sheet is an example of this case. It is clear that when a sheet is crumpled by closing then opening, its surface area remains constant and thus its projection lengths decrease due to the surface roughness. To examine such a case, three rippled graphene sheets with constant area, equal to 1 nm^2, are considered with different frequencies of the surface roughness. In these cases, because the graphene area is kept constant, variation of surface roughness causes the change in projection lengths, e.g., graphene sheets with $n = 3$, $n = 11$ and $n = 21$ have projection lengths equal to 0.9972, 0.9654 and 0.8979, respectively. The variation of the equivalent stiffness is depicted in Fig. 5 for constant area graphene sheets with different roughness frequencies. It can be seen that the bending stiffness increases with increase in the frequency and it does not converge.

6. Pure geometrical model for an equivalent stiffness

In the previous sections, the rippling of graphene has been modeled by an initial geometry. As the graphene surface becomes wavy, its moment of inertia changes and this causes increase in its stiffness. Thus, one can also find an equivalent stiffness of a wrinkled graphene for small roughness with pure geometrical considerations in addition to the previous method. Consider a graphene with an initial roughness like Eq. (1), then the bending stiffness for a differential element of a non-flat shape can be written as

$$\mathrm{d}D_{ij} = \int_{u^0-l_3/2}^{u^0+l_3/2} Q_{ij}x_3^2\,\mathrm{d}x_3 \tag{16}$$

As it can be seen the interval of the integral changes because of the initial deflection u^0. Since u^0 is not constant through the surface, the integral and therefore the bending stiffness changes at every point. In order to obtain an equivalent stiffness for a rippled graphene, the average stiffness through the surface is calculated as

$$D_{ij} = \frac{1}{S}\int_S\int_{u^0-l_3/2}^{u^0+l_3/2} Q_{ij}x_3^2\,\mathrm{d}x_3\,\mathrm{d}s = \frac{Q_{ij}l_3^3}{12} + \frac{Q_{ij}l_3}{S}\int_{-l_2/2}^{l_2/2}\int_{-l_1/2}^{l_1/2} u^{0^2}\sqrt{1+\left(\frac{\mathrm{d}u^0}{\mathrm{d}x}\right)^2+\left(\frac{\mathrm{d}u^0}{\mathrm{d}y}\right)^2}\,\mathrm{d}x_1\,\mathrm{d}x_2 \tag{17}$$

where $\mathrm{d}s$ is an area element and u^0 is the initial deflection. Also, S is the area of the wrinkled graphene as

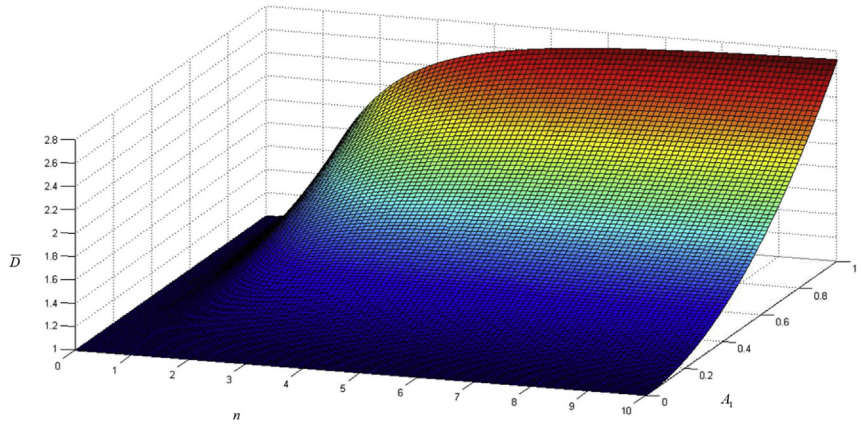

Fig. 3. Variation of the equivalent bending stiffness ratio of a rippled graphene with respect to surface parameters ($e_0a = 0.1l$, $\nu = 0.149$).

$$S = \int_{-l_2/2}^{l_2/2} \int_{-l_1/2}^{l_1/2} \sqrt{1 + \left(\frac{du^0}{dx}\right)^2 + \left(\frac{du^0}{dy}\right)^2}\, dx_1\, dx_2 \tag{18}$$

By substituting Eq. (1) into Eq. (17) and calculating the integrals, an equivalent bending stiffness is obtained for a rippled graphene by a pure geometrical model.

7. Numerical results

In order to verify the accuracy of the formulations, the results are compared with available results for classical ($e_0a = 0$) corrugated plate. The stiffness of sinusoidal or cosine corrugated plate in one direction was approximated in literature with an orthotropic model [41]. In order to compare with this model, $n_{21} = 0$ has been considered in our model. The results are compared in Fig. 6 with a sinusoidal corrugated plate with the additional rigidities and it can be concluded that formulations have a good accuracy.

For numerical simulations, the following material properties are considered for the graphene layer [26,38].

$$\widehat{D}_{11} = 0.234 \text{ nN nm} = 1.46 \text{ eV}; \quad \widehat{D}_{22} = 0.229 \text{ nN nm} = 1.43 \text{ eV}; \quad \nu_{12} = 0.149; \quad \nu_{21} = 0.145 \tag{19}$$

where $\widehat{D}_{ii} = E_{ii}l_3^3/12(1 - \nu_{12}\nu_{21})$ is the bending modulus of a flat graphene. Also, the nonlocal parameter and external loading are considered equal to $e_0a = 0.25$ nm and $P = 10E_{11}(l_3/l_1)^4$, respectively.

In order to find the linearity range of graphene deflection, the maximum deflection of a flat graphene versus external load is shown in Fig. 7. It can be seen that deflection of graphene is completely nonlinear especially for large values of external pressure. It can be concluded that for higher deflection, the in-plane stretching–bending effects become more significant and they play an important role in bending of graphene. Also, it can be seen that the graphene has a hardening stiffness. Thus, in order to capture these effects and obtain more accurate results from large deflection, the nonlinear effects should be considered.

To capture the stiffness of graphene for large deflection, the gradient of the force–displacement curve is calculated as

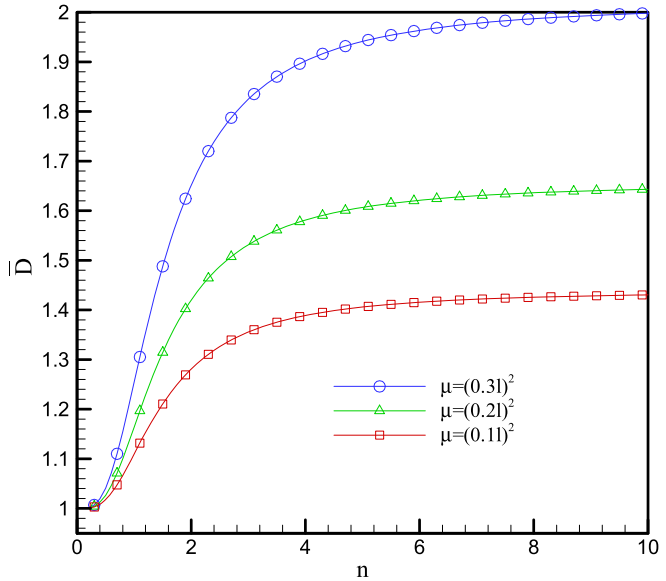

Fig. 4. Variation of equivalent bending stiffness versus frequency of surface rippling ($A_1 = 0.5$, $\nu = 0.149$).

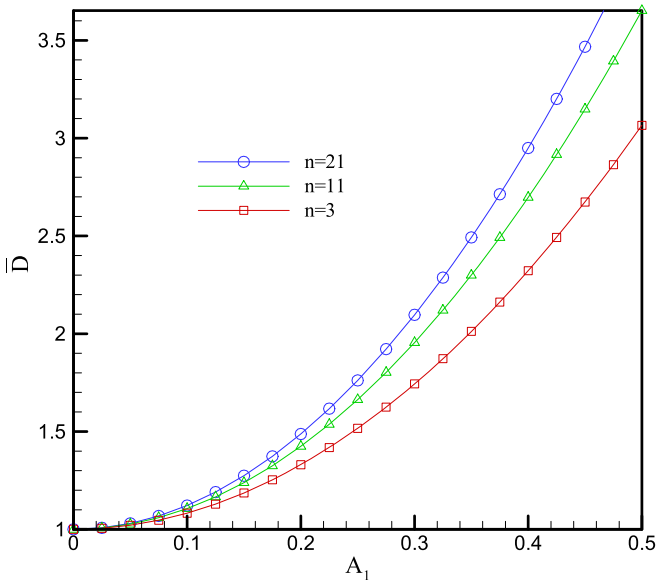

Fig. 5. Variation of equivalent stiffness for different rippled graphene with constant surface area ($e_0a = 0.3$, $\nu = 0.149$).

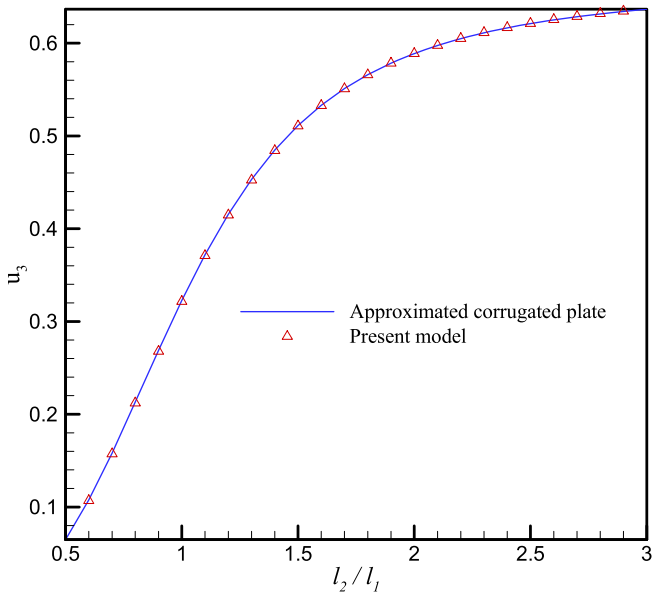

Fig. 6. Comparison of the maximum deflection with one directional corrugated model ($E_{11} = E_{22} = 3.85$ kPa, $\nu = 0.148$, $A_1 = 0.1l_3$).

$$\kappa = \frac{\partial p}{\partial u_3} \tag{20}$$

The variation between this stiffness to that of a flat graphene is shown in Fig. 8 (for one and two terms uneven surface). Since we have considered the nonlinear case, the stiffness is not constant and depends on the external force. As it can be seen stiffness of a rippled graphene has hardening effect and increases with respect to the external force. It can also be seen that hierarchical rippling can further increase the stiffness of a rippled graphene. Thus, it can be concluded that the effect of surface amplitude on the graphene stiffness is much more pronounced than the effect of surface frequency.

The maximum non-dimensional central transverse deflection u_3 for different values of initial wave number is presented in Table 1. A square graphene with dimension of 1 nm is considered and the amplitudes of rippling waves are assumed as $A_1 = 2l_3$ and $A_2 = l_3/4$. The value in parenthesis is the decrease percentage of non-dimensional deflection from that of flat graphene which is 0.45. It can be seen that the first wave numbers (n_{11}, n_{21}) have considerable

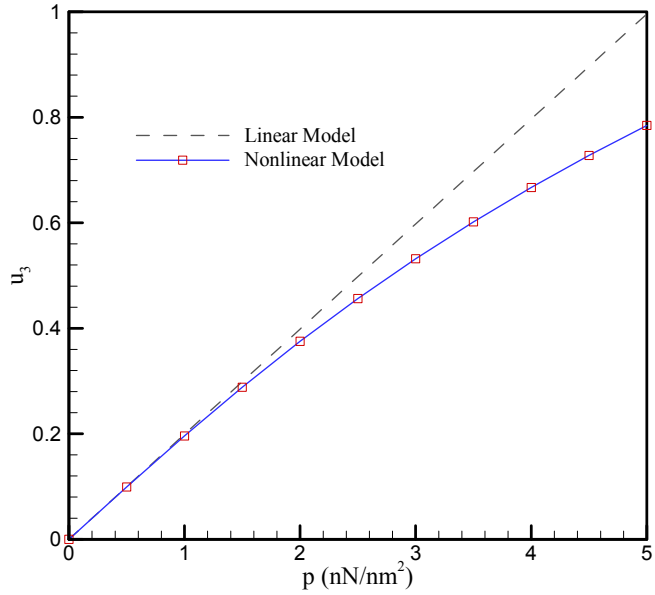

Fig. 7. Variation of transverse deflection of flat graphene versus the external pressure.

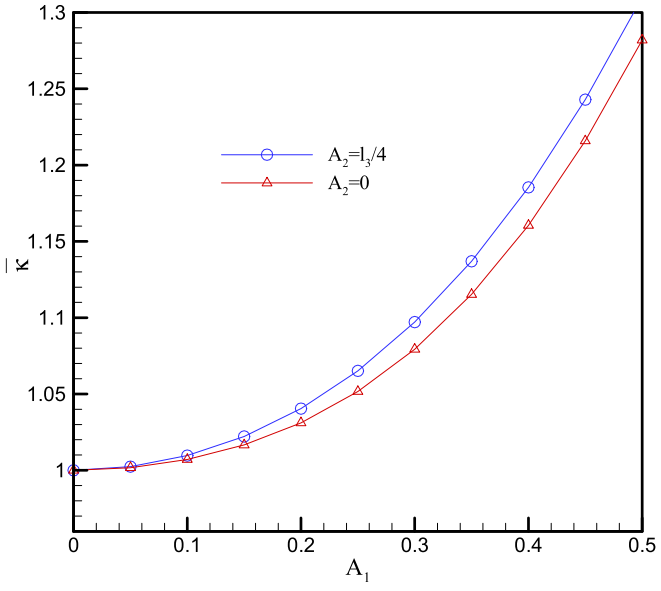

Fig. 8. Variation of stiffness of rippled graphene versus the surface amplitude ($n_{12} = n_{22} = 101$).

Table 1
Maximum transverse deflection of graphene (u_3) for different values of wave number ($A_1 = 2l_3$, $A_2 = l_3/4$).

$n_{11} = n_{21}$	$n_{12} = n_{22}$		
	0	51	101
3	0.434 (3.5%)	0.4341 (3.56%)	0.4341 (3.56%)
5	0.432 (3.97%)	0.4319 (4.04%)	0.4319 (4.04%)
11	0.4311 (4.22%)	0.4308 (4.29%)	0.4308 (4.29%)
101	0.4308 (4.29%)	0.4305 (4.35%)	0.4259 (5.38%)

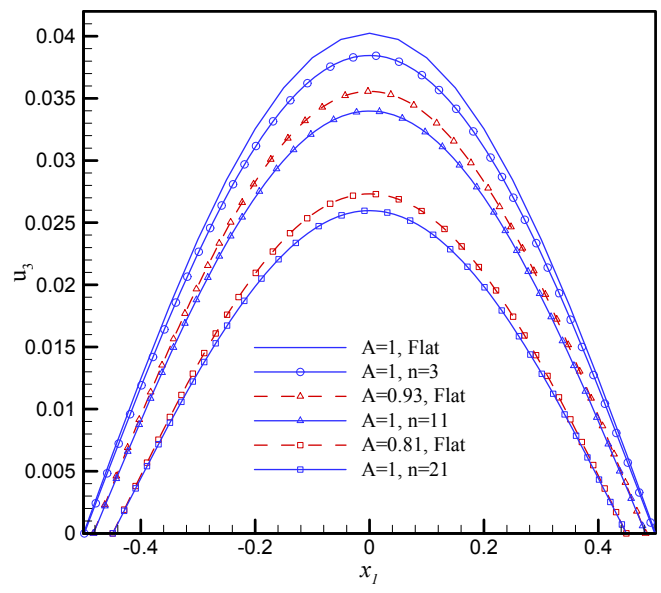

Fig. 9. Transverse deflection of graphene for different initial surfaces and lengths.

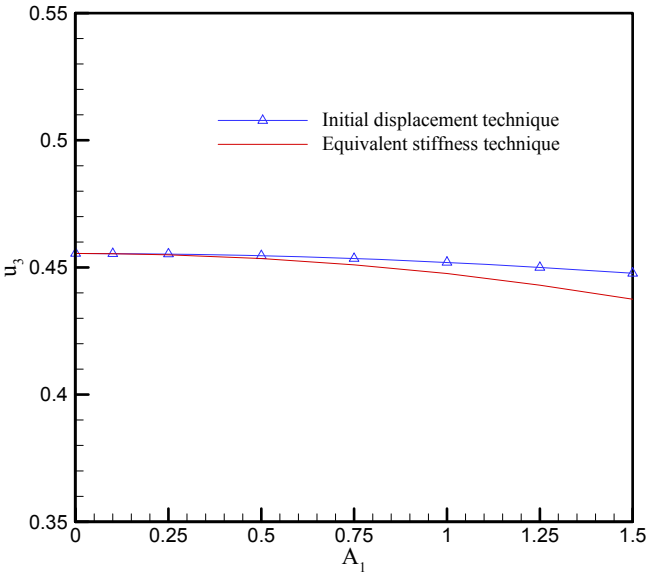

Fig. 10. Variation of maximum deflection of graphene with respect to initial rippling for the two proposed methods ($n_{11} = n_{21} = 3$, $A_2 = 0$, $e_0a = 0$).

effect on the stiffness of graphene. As the flat surface of graphene is changed to uneven surface, its moment of inertial rapidly increases and it causes an increase in stiffness. It can be seen that this effect is more significant for lower wave numbers. A graphene with higher values of wave numbers can be regarded as an opened crumpled graphene. It can be seen that the roughness of graphene surface significantly increases its stiffness.

When a flat surface of graphene changes to uneven surface, length of graphene decreases due to constant surface area. Transverse deflection of middle line of graphene versus x_1 direction is depicted in Fig. 9 for a flat and uneven surface with constant area and constant length. It can be seen that for an opened crumpled graphene with constant surface area, the decrease of the transverse deflection is very considerable. As compared to graphene sheets with constant length but different surface area, the effect of length change on the stiffness is more than that of roughness for an opened crumpled graphene.

In order to define the maximum value of roughness amplitude, in which the equivalent pure geometrical stiffness is a good approximation of the real stiffness, the variation of maximum deflection is depicted in Fig. 10 for both of the presented approaches. The equivalent geometrical stiffness has a suitable accuracy only for small rippling amplitudes, e.g., for initial dimensionless amplitude of 1.5, the error becomes about 4.4%.

8. Conclusions

The effect of rippling on the bending stiffness of graphene has been presented. Rippling has been modeled by cosine functions with arbitrary amplitudes and frequencies. In order to obtain more accurate results for large deflection, nonlinear strain–displacement relations have been used according to von Karman assumptions. The governing equilibrium equations have been determined by considering the small scale effect and then solved using the Galerkin's method. Effects of initial roughness, small length scale and dimension on the stiffness of graphene have been discussed in details. The results reveal that the rippling strongly increases the stiffness of graphene and affects the behavior of small length scale. It has been concluded that the effect of changing length on stiffness is more pronounced than changing roughness for an opened crumpled graphene. It has been proved that the increase in stiffness due to uneven surface is more considerable when the small length scale is considered. This study can help design of graphene with higher bending stiffness.

Acknowledgment

The support for this work, provided by the Iran Nanotechnology Initiative Council, is gratefully acknowledged. NMP is supported by the European Research Council (ERC StG Ideas 2011 BIHSNAM n. 279985 on “Bio-Inspired hierarchical super-nanomaterials”, ERC PoC 2013-1 REPLICA2 n. 619448 on “Large-area replication of biological anti-adhesive nanosurfaces”, ERC PoC 2013-2 KNOTOUGH n. 632277 on “Super-tough knotted fibres”), by the European Commission under the Graphene Flagship (WP10 “Nanocomposites”, n. 604391) and by the Provincia Autonoma di Trento (“Graphene Nanocomposites”, n. S116/2012-242637 and reg. delib. n. 2266).

Appendix A

The coefficients of the governing equilibrium equations are obtained in terms of the mechanical properties of graphene as

$$A_{11} = \frac{Q_{22}}{l_3\left(Q_{11}Q_{22} - Q_{12}^2\right)}, \quad A_{12} = -\frac{Q_{12}}{l_3\left(Q_{11}Q_{22} - Q_{12}^2\right)},$$
$$A_{22} = \frac{Q_{11}}{l_3\left(Q_{11}Q_{22} - Q_{12}^2\right)}, \quad A_{33} = \frac{1}{l_3 Q_{33}},$$
$$D_{11} = \frac{l_3^3 Q_{11}}{12}, \quad D_{12} = \frac{l_3^3 Q_{12}}{12}, \quad D_{22} = \frac{l_3^3 Q_{22}}{12}, \quad D_{33} = \frac{l_3^3 Q_{33}}{12} \tag{A.1}$$

where the plane-stress constants are defined as

$$Q_{11} = \frac{E_{11}\left(\cos^4\theta + 2\nu_{21}\sin^2\theta\cos^2\theta\right) + E_{22}\sin^4\theta}{1-\nu_{12}\nu_{21}} + 4G_{12}\sin^2\theta\cos^2\theta$$
$$Q_{12} = \frac{E_{11}\left(\sin^2\theta\cos^2\theta + \nu_{21}\sin^4\theta + \nu_{21}\cos^4\theta\right) + E_{22}\sin^2\theta\cos^2\theta}{1-\nu_{12}\nu_{21}} - 4G_{12}\sin^2\theta\cos^2\theta$$
$$Q_{22} = \frac{E_{11}\left(\sin^4\theta + 2\nu_{21}\sin^2\theta\cos^2\theta\right) + E_{22}\cos^4\theta}{1-\nu_{12}\nu_{21}} + 4G_{12}\sin^2\theta\cos^2\theta \tag{A.2}$$
$$Q_{33} = \frac{E_{11}\left(\sin^2\theta\cos^2\theta - 2\nu_{21}\sin^2\theta\cos^2\theta\right) + E_{22}\sin^2\theta\cos^2\theta}{1-\nu_{12}\nu_{21}} + G_{12}\left(\cos^2\theta - \sin^2\theta\right)$$

where θ denotes the chiral angle, E_{11} and E_{22} are Young's modulus in the direction and perpendicular of chiral vector, respectively. Also, G_{12} and ν are the shear modulus and Poisson's ratio of the graphene sheet, respectively.

References

[1] Lee C, Wei X, Kysar JW, Hone J. Measurement of the elastic properties and intrinsic strength of monolayer graphene. Science 2008;321:385–8.
[2] Balandin AA, Ghosh S, Bao W, Calizo I, Teweldebrhan D, Miao F, et al. Superior thermal conductivity of single-layer graphene. Nano Lett 2008;8:902–7.
[3] Fasolino A, Los JH, Katsnelson MI. Intrinsic ripples in graphene. Nat Mater 2007;6:858–61.
[4] Kim K, Lee Z, Malone BD, Chan KT, Alemán B, Regan W, et al. Multiply folded graphene. Phys Rev B 2011;83:245433.
[5] Meyer JC, Geim AK, Katsnelson MI, Booth TJ, Roth S. The structure of suspended graphene sheets. Nature 2007;446:60–3.
[6] Sung-Chiun S, Jia-Lin T. Characterizing thermal and mechanical properties of graphene/epoxy nanocomposites. Compos Part B Eng 2014;56:691–7.
[7] Atalaya J, Isacsson A, Kinaret JM. Continuum elastic modeling of graphene resonators. Nano Lett 2008;8:4196–200.
[8] Arash B, Wang Q. A review on the application of nonlocal elastic models in modeling of carbon nanotubes and graphenes. Comput Mater Sci 2012;51:303–13.
[9] Rafiee R, Maleki Moghadam R. On the modeling of carbon nanotubes: a critical review. Compos Part B Eng 2014;56:435–49.
[10] Tserpes KI, Papanikos P. Finite element modeling of single-walled carbon nanotubes. Compos Part B Eng 2005;36:468–77.
[11] Lu X, Hu Z. Mechanical property evaluation of single-walled carbon nanotubes by finite element modeling. Compos Part B Eng 2012;43:1902–13.
[12] Baykasoglu C, Kirca M, Mugan A. Nonlinear failure analysis of carbon nanotubes by using molecular-mechanics based models. Compos Part B Eng 2013;50:150–7.
[13] Murmu T, Adhikari S. Nonlocal vibration of bonded double-nanoplate-systems. Compos Part B Eng 2011;42:1901–11.
[14] Mohammadi M, Ghayour M, Farajpour A. Free transverse vibration analysis of circular and annular graphene sheets with various boundary conditions using the nonlocal continuum plate model. Compos Part B Eng 2013;45:32–42.
[15] Karličić D, Adhikari S, Murmu T, Cajić M. Exact closed-form solution for nonlocal vibration and biaxial buckling of bonded multi-nanoplate system. Compos Part B Eng 2014;66:328–39.
[16] Mohammadi M, Farajpour A, Moradi A, Ghayour M. Shear buckling of orthotropic rectangular graphene sheet embedded in an elastic medium in thermal environment. Compos Part B Eng 2014;56:629–37.
[17] Radić N, Jeremić D, Trifković S, Milutinović M. Buckling analysis of double-orthotropic nanoplates embedded in Pasternak elastic medium using nonlocal elasticity theory. Compos Part B Eng 2014;61:162–71.
[18] Narendar S, Gopalakrishnan S. Nonlocal continuum mechanics based ultrasonic flexural wave dispersion characteristics of a monolayer graphene embedded in polymer matrix. Compos Part B Eng 2012;43:3096–103.
[19] Jomehzadeh E, Saidi AR. Decoupling the nonlocal elasticity equations for three dimensional vibration analysis of nano-plates. Compos Struct 2011;93:1015–20.
[20] Xu X, Liao K. Molecular and continuum mechanics modeling of graphene deformation. Mater Phys Mech 2001;4:148–51.
[21] Lu Q, Huang R. Nonlinear mechanics of single-atomistic–atomic layer graphene sheets. Int J Appl Mech 2009;1:443–67.
[22] Duan WH, Wang CM. Nonlinear bending and stretching of a circular graphene sheet under a central point load. Nanotechnology 2009;20:075702.
[23] Rezaei Mianroodi J, Amini Niaki S, Naghdabadi R, Asghari M. Nonlinear membrane model for large amplitude vibration of single layer graphene sheets. Nanotechnology 2011;22:305703.
[24] Wang Q. Simulations of the bending rigidity of graphene. Phys Lett A 2010;373:1180–3.
[25] Shen L, Shen HS, Zhang CL. Nonlocal plate model for nonlinear vibration of single layer graphene sheets in thermal environments. Comput Mater Sci 2010;48:680–5.
[26] Shen HS, Shen L, Zhang CL. Nonlocal plate model for nonlinear bending of single-layer graphene sheets subjected to transverse loads in thermal environments. Appl Phys A 2011;103:103–12.
[27] Jomehzadeh E, Saidi AR. A study on large amplitude vibration of multilayered graphene sheets. Comput Mater Sci 2011;50:1043–51.
[28] Pereira VM, Castro Neto AH, Liang HY, Mahadevan L. Geometry, mechanics, and electronics of singular structures and wrinkles in graphene. Phys Rev Lett 2010;105:156603.
[29] Wang CY, Mylvaganam K, Zhang LC. Wrinkling of monolayer graphene: a study by molecular dynamics and continuum plate theory. Phys Rev B 2009;80:155445.
[30] Surya VJ, Iyakutti K, Emelda K. Ripples in graphene: a theoretical analysis using two dimensional vibrating membrane model. In: Solid State Physics Proceedings of the 55th DAE Solid State Physics Symposium, vol. 1349; 2010. p. 297–8.
[31] Bonilla LL, Carpio A. Model of ripples in graphene. Phys Rev B 2012;86:195402.
[32] Berry MV, Lewis ZV. On the Weierstrass–Mandelbrot fractal function. Proc R Soc A 1980;370:459–84.
[33] Kirchhoff GR. Uber das gleichgewichi und die bewegung einer elastishem scheibe. J Reine Angew Math 1850;40:51–88.
[34] Von Karman Th. Encyklop die der mathematischen. Wissenschaften 1910:5–6.
[35] Eringen AC, Edelen DGB. On nonlocal elasticity. Int J Eng Sci 1972;10:233–48.
[36] Eringen AC. On differential equations of nonlocal elasticity and solutions of screw dislocation and surface waves. J Appl Phys 1983;54:4703–10.
[37] Jomehzadeh E, Saidi AR, Pugno NM. Large amplitude vibration of a bilayer graphene embedded in a nonlinear polymer matrix. Phys E Low-Dimens Syst Nanostr 2012;44:1973–82.
[38] Jomehzadeh E, Afshar MK, Galiotis C, Shi X, Pugno NM. Nonlinear softening and hardening nonlocal bending stiffness of an initially curved monolayer graphene. Int J Non-Linear Mech 2013;56:123–31.
[39] Vendhan CP, Das YC. Application of Rayleigh–Ritz and Galerkin methods to non-linear vibration of plates. J Sound Vib 1975;39:147–57.
[40] Ventsel E, Krauthammer T. Thin plates and shells: theory, analysis, and applications. Marcel Dekker, Inc; 2001. p. 51.
[41] Reddy JN. Theory and analysis of elastic plates. Taylor & Francis; 1999. p. 136.